INL/CON-12-26061
PREPRINT

Mechanisms of Gas Precipitation in Plasma-Exposed Tungsten

20th International Conference on Plasma-Surface Interactions 2012

R. D. Kolasinski
D. F. Cowgill
D. C. Donovan
M. Shimada
W. R. Wampler

May 2012

The INL is a
U.S. Department of Energy
National Laboratory
operated by
Battelle Energy Alliance

Mechanisms of gas precipitation in plasma-exposed tungsten

R. D. Kolasinski*,[(a)], D. F. Cowgill[(a)], D. C. Donovan[(a)], M. Shimada[(b)], and W. R. Wampler[(c)]

[(a)]*Sandia National Laboratories, Hydrogen and Metallurgical Science Department, Livermore, CA 94551 USA*

[(b)]*Idaho National Laboratory, Fusion Safety Program, P.O. Box 1625, Idaho Falls, ID 83415 USA*

[(c)]*Sandia National Laboratories, Radiation-Solids Interactions Department, Albuquerque, NM 87185 USA*

Abstract – Precipitation in subsurface bubbles is a key process that governs how hydrogen isotopes migrate through and become trapped within plasma-exposed tungsten. We describe a continuum-scale model of hydrogen diffusion in plasma-exposed materials that includes the effects of precipitation. The model can account for bubble expansion via dislocation loop punching, using an accurate equation of state to determine the internal pressure. This information is used to predict amount of hydrogen trapped by bubbles, as well as the conditions where the bubbles become saturated. In an effort to validate the underlying assumptions, we compare our results with published positron annihilation and thermal desorption spectroscopy data, as well as our own measurements using the tritium plasma experiment (TPE).

PSI-19 keywords: tungsten, bubbles and blisters, hydrogen inventory, diffusion

PACS codes: 61.72.Qq, 52.40.Hf, 81.05.Bx

Corresponding author address:

Robert D. Kolasinski

Sandia National Laboratories

P.O. Box 969, MS 9161

Livermore, CA 94550 USA

e-mail: rkolasi@sandia.gov

Presenting author: (Same as corresponding author.)

I. Introduction

Hydrogen migration and trapping in plasma-exposed tungsten are complex processes, and developing models which capture the correct physical mechanisms is a challenging task. A review of the published experimental database reveals that a wide range of trapping mechanisms have been previously observed [1]. Of particular interest is precipitation, where atomic hydrogen in solution recombines into H_2(g) upon encountering sub-surface voids and bubbles [2]. These precipitates have the capacity to trap a large amount of hydrogen at shallow depths. Upon mechanical failure of the bubble structure (typically through fissures leading to the surface) the trapped hydrogen gas is able to escape [3]. This has the benefit of reducing the total retention in plasma facing materials by preventing diffusion to deeper trap sites.

Being able to more rigorously predict the amount of hydrogen trapped in the bubbles would be particularly helpful for estimating tritium inventory in ITER. The broad distribution of bubble sizes possible with different material microstructures and plasma conditions (e.g. exposure to mixtures of both He and H) introduces challenges to predicting how efficiently the bubbles trap hydrogen under different conditions. These processes are being addressed by a number of researchers using density functional theory (DFT), molecular dynamics (MD), and kinetic Monte Carlo approaches [4]. Such models provide a wealth of fundamental insight into basic physical processes, but tend to be restricted to small spatial domains over very limited time scales. A number of general-purpose continuum-scale diffusion codes, such as TMAP7 [5], are in wide use within the magnetic fusion community and have been applied to modeling thermal desorption spectroscopy from plasma-exposed materials. These models allow point defects to be simulated, but cannot yet account for precipitation. Hence, care must be taken when applying them to situations where the effect of bubbles is important.

Incorporating approximations to atomic-scale effects into a simpler model offers a pathway to simulate trapping in bubbles for practical experimental conditions. In a previous study [6], we developed the basic theoretical framework needed to model precipitation in tungsten at a continuum-scale, extensively leveraging Cowgill's prior models of ^{3}He bubble growth in metal tritides [7]. Using this approach, we were able to identify the conditions amenable to hydrogen precipitation using the

assumption that the bubbles expand by dislocation loop punching. In this article, we describe several extensive modifications to our model, including an improved treatment of trapping by bubbles. In an effort to refine and validate the model, we compare simulated test cases with analytical calculations, as well as published positron annihilation measurements. We also discuss initial results from our experimental work, including exposures of ITER-grade and warm-rolled tungsten sample materials using the tritium plasma experiment (TPE).

II. Continuum-scale model and underlying assumptions

From the perspective of hydrogen precipitation in tungsten, the most important parameter is the enthalpy of solution, H_s, which is 1.04 eV relative to ½ H_2(g) [8]. This indicates that introducing hydrogen into solution sites within tungsten is a strongly endothermic process. Thus, under most conditions hydrogen migrating through the lattice could achieve a lower energy state by recombining upon encountering a void. We developed our continuum-scale model with the objective of simulating controlled laboratory experiments, keeping in mind that any simplifications can later be relaxed to address a more realistic environment. Many of the major underlying assumptions are described in Ref. [6], and only a summary is presented here. We consider 1-D hydrogen diffusion with a uniform temperature distribution, T. The simplified governing equation that includes trapping and precipitation is

$$\partial u(x,t)/\partial t = D(T(t))\,\partial^2 u(x,t)/\partial x^2 - q_T(x,t) - q_B(x,t) + \Phi(x,t)$$

where $u(x,t)$ is the concentration of hydrogen in solution, and D is the diffusivity. The flow of hydrogen into and out of satruable traps and bubbles is dictated by $q_T(x,t)$ and $q_B(x,t)$ respectively, whereas the implanted flux is indicated by $\Phi(x,t)$. Note that because we assume that $\partial T/\partial x = 0$, concentration gradients arising from the Ludwig-Soret effect may be neglected. We also ignore strain effects on hydrogen diffusion.

During ion implantation, H is injected directly into solution sites within the lattice. A key consideration is the surface boundary condition which governs how the implanted hydrogen leaves the surface. Recombination coefficients for the W+H system have been measured by several researchers,

but the spread in these values is 10 orders of magnitude [1]. Likely contributing to this is the effect of adsorbed impurities, which even at small concentrations decrease the recombination rate drastically. Experimental studies that are successful in controlling surface impurities report recombination consistent with a model based on second-order kinetics [9]. When extrapolated to W, these results suggest fast recombination, consistent with diffusion-limited release from the surface. For this reason, we assume boundary condition of $u(0,t) = 0$ for the front surface.

As discussed in further detail in Ref. [6], we treat point defects (saturable traps) separately from bubbles. Analytical expressions for the flow of hydrogen into point defects, $q_t(x,t) = \partial u_t(x,t)/\partial t$, have been developed by several authors; we have implemented a model similar to the one used in TMAP7. (We refer the reader to Ref. [5] for more details.) To efficiently calculate the flow of H into bubbles, we use a widely used analytical approach developed by Ham [10], given by the following straightforward expression:

$$q_B(x,t) = \partial u_B(x,t)/\partial t = 4\pi D(t) r_B(x,t) N_B(x)\left[u(x,t) - u_{eq}(x,t)\right]$$

where r_B is the bubble radius, u_B is the concentration trapped in bubbles, N_B is the number density of bubbles within the lattice, and u_{eq} is the equilibrium concentration in solution evaluated at the bubble surface. Note that u_{eq} may be determined by calculating the fugacity of the high-pressure gas within the bubble using a realistic equation of state and assuming Sievert's Law is satisfied at the bubble interface. When $u(x,t) < u_{eq}(x,t)$ the direction of flow is out the bubble, thereby enabling the simulation of thermal desorption by this expression.

Ham's elegant expression is derived by determining the solute species concentration surrounding an array of evenly-spaced, spherical precipitates using an eigenfunction expansion. If r_B is assumed to be much smaller than the inter-bubble spacing, only the first term of this expansion will be important, which simplifies the resulting expression considerably. In addition, our expression for q_B also assumes that any temporal variations in the mobile concentration far from the precipitate are small, so that quasi-equilibrium is always satisfied. (Given the high diffusivity of hydrogen in tungsten, this is generally not a significant problem for most conditions encountered in laboratory experiments.)

Calculating the amount of hydrogen accumulated in bubbles and traps involves solving coupled parabolic PDE's. For this purpose, we used the method of lines approach, where only the spatial derivative is discretized. For a given segment i, the system of equations becomes:

$$du_i(t)/dt = D_i \frac{u_{i-1} - 2u_i + u_{i+1}}{{\Delta x_i}^2} - q_{T_i}(t) - q_{B_i}(t) + \Phi_i(t)$$

This converts the PDE into a coupled set of ordinary differential equations which can be rearranged in the following form:

$$G(u(t), u_T(t), u_B(t), t) = 0$$

To solve this system, we used the differential algebraic equation (DAE) solver DASPK developed by Petzhold [11]. This is a more advanced version of the DASSL routine developed specifically for stiff DAE systems. The solver iteratively attempts to minimize the value of G subject to accuracy constraints.

III. Chemical equilibrium and equation of state

Determining whether hydrogen will flow into subsurface bubbles requires calculating the solution concentration that will be in equilibrium the precipitated gas. One must therefore determine the fugacity of the gas in the bubbles accurately using an equation of state that takes into account non-ideal gas effects at high pressure. Fig. 1 shows a comparison of the existing experimental database [12-14] and curve fits [15-16] for the behavior of hydrogen at high pressure at ambient temperature. Note that the ideal gas law approximation diverges in the pressure range 10-100 MPa.

The equation of state proposed by Tkacz [16] appears to be quite accurate over a wide pressure range:

$$v = Ap^{-1/3} + Bp^{-2/3} + Cp^{-4/3} + (D + ET)p^{-1}$$

Note that for H_2, $A = 176.330$, $B = -633.675$, $C = -304.574$, $D = 731.393$, and $E = 8.59805$. It is important to keep in mind that while specific volume is easily expressed in terms of pressure, the inverse relationship cannot be easily expressed in a simple, closed-form equation. In addition, because

Tkacz's equation uses a polynomial fitting function, it provides erratic results far outside of its intended range of use. This is not immediately obvious from Fig. 1, and therefore care must be taken when applying this fit. For this reason, we transition to the equation of state developed by San Marchi et al. [15] at intermediate pressures, as it asymptotes to the ideal gas law.

In small hydrogen bubbles, pressures > 1 GPa are needed for dislocation loop punching. The magnitude of this pressure is rather striking, particularly because this is near the point where hydrogen forms a molecular solid. (Early experiments with diamond anvil high-pressure cells found solidification at 5.7 GPa and 25 °C; later x-ray measurements confirmed the structure to be hexagonal-close-packed with a H_2 molecule at each lattice point [14].) This highlights the extreme conditions encountered in plasma-exposed materials, but causes one to question whether the pressure in hydrogen bubbles in tungsten could realistically grow to such high levels. We point out that such pressures are not unprecedented, particularly given prior observations of ^{3}He solidification in PdT_x with nuclear-magnetic-resonance (NMR) analysis [17]. Because it is straightforward to incorporate into a continuum model, we will focus primarily on the dislocation loop-punching mechanism described above.

IV. Results and Discussion

To test the underlying assumptions incorporated into our simulations, we considered a series of thermal desorption spectroscopy (TDS) and positron annihilation (PA) experiments by Van Veen et al. [18]. To summarize their work, W(100) single crystals were initially damaged with 6 MeV protons. The beam energy was adjusted to produce a uniform concentration of vacancies (4×10^{-5} /W) up to a depth of 35 μm. After heating to 1200 K for 15 min., voids formed throughout this volume at a concentration of 10^{-6} /W. The average void diameter corresponded to approx. 1 nm (~30 – 50 vacancies, as determined by PA.) Afterward, the samples were bombarded with 2 keV H_2^+ with an incident flux of $\Phi=1.25\times10^{18}$ $m^{-2}s^{-1}$; the authors considered doses of 10^{22} m^{-2} and 10^{23} m^{-2}. All exposures were performed at 350 K.

Many experimental studies propose a model for the energetics that includes the existence of point defects such as vacancies (H_t=1.4 eV), and surface traps corresponding to the dissociation enthalpy of hydrogen chemisorbed on the interior wall of a void (1.8-2.1 eV) [1]. The ability of our model to predict the equilibrium fraction of the traps filled as a function of temperature is therefore crucial. As illustrated in Fig. 2(a) for 1.4 eV traps, our model is in accord with an analytical expression from Ref. [2]. It is also useful to consider the special case where the concentration of traps is much larger than the mobile concentration at the depth of implantation, i.e. $N_t \gg u(r,t)$, where r is the range of the implanted ions. Under these conditions, the traps will be completely filled up to an interface defined by $x = \sqrt{2Dtu(r,t)/N_t}$, and empty thereafter. (We refer the reader to Ref. [2] for more details.) Through a rearrangement of this expression, it is straightforward to calculate the total retention as a function of dose. As we will describe below, such a model can also be readily adapted to simulating the filling of voids, providing an analytical check for our model. To simulate 2 keV H_2^+ (or 1 keV H^+) ion bombardment, we calculated an implantation range of 9 nm using TRIM [19]. Consistent with the PA measurements, we assume that the vacancies produced by the 6 MeV proton irradiation became mobile and combined to form voids during the 1200 K anneal. With this in mind, we populated a region within 35 μm of the surface uniformly with voids.

Consistent with the findings of Van Veen et al., we found that for the ion fluxes described in Ref. [18], 1 nm dia. voids were not able to accumulate enough hydrogen to punch dislocation loops. Instead, equilibrium with the hydrogen in solution was achieved for 40 H/bubble. This is somewhat less than the ~100-200 H/bubble determined by Van Veen et al. from their PA measurements. We suspect this is partially due to their reliance on an older equation of state for high pressure H when fitting their PA measurements. In any case, a slight adjustment to the average void diameter (to 1.5 nm) brings the number of hydrogen that can be accommodated at saturation to 150 H/bubble, which is very much in accord with their measurements. To assess the total amount of hydrogen trapped within the voids, Van Veen et al. used thermal desorption spectroscopy. For doses of 10^{22} m^{-2} and 10^{23} m^{-2}, the retention was determined to be 1.2×10^{20} m^{-2} and 2.0×10^{20} m^{-2}, respectively. We were able to

obtain comparable values by adjusting the void concentration to 2 appm. This is certainly within the uncertainty of the PA measurements.

Under the conditions described above, the voids behave essentially like saturable traps. We should point out that it is conceivable that one could match the aforementioned retention results by simply assuming an evenly dispersed population of point defects with dissociation energies ranging between of 1.8-2.1 eV, as illustrated in Fig. 2(b). However, the model we have proposed here presents a much more accurate depiction of the actual physical processes involved with trapping within bubbles. As illustrated in Fig. 2(c), the voids are completely filled up to an interface and then empty afterward, consistent with the behavior described previously.

These initial results certainly provide evidence that a continuum-scale approach could be applied to accurately modeling trapping by bubbles in tungsten. However several key obstacles still remain. The next step in developing this model is applying it to the growth of large precipitates in more realistic laboratory conditions and using this information to eventually predict total tritium inventory in ITER. A key challenge associated with this will be determining how to include the effects of the micro-scale structure of the material into the model. To illustrate the effect of material processing, consider Fig. 3 which shows a comparison of post-mortem surface morphology between ITER-grade (A.L.M.T. Corp.) and warm-rolled (PLANSEE) tungsten samples. Both materials were exposed to 100 eV D_2^+ ions in the tritium plasma experiment (TPE) located at Idaho National Laboratory. (Please see Ref. [20] for a more comprehensive description of the experimental hardware.) In each case, the samples were electrical discharge machined from the raw material, polished to an RMS surface roughness of 0.2 μm, and then stress relieved in ultra-high vacuum at 1000 °C for 1 hr. The exposure conditions for both samples were nearly identical, as indicated in Fig. 3. Nevertheless, the two surfaces have drastically different surface morphologies. Whereas the ITER tungsten is characterized by small surface bubbles < 5 μm in dia., the warm-rolled tungsten contains blisters in excess of 50 μm. In the case of the warm-rolled tungsten, the grains are elongated parallel to the surface, providing a well-defined boundary for subsurface cracks to form [6]. In the case of the ITER-grade samples, the

grain orientation is perpendicular to the surface, which is not conducive to such large-scale delaminations.

V. Acknowledgements

We thank Dean Buchenauer, Chris San Marchi, and Rion Causey for helpful discussions regarding this work. Sandia National Laboratories is a multi-program laboratory managed and operated by Sandia Corporation, a wholly owned subsidiary of Lockheed Martin Corporation, for the U.S. Department of Energy's National Nuclear Security Administration under contract DE-AC04-94AL85000.

References

[1] R. A. Causey, *J. Nucl. Mater.* **300** (2002) 91.

[2] W. R. Wampler and R. P. Doerner, *Nucl. Fusion* **49** (2009) 115023.

[3] A. Manhard, U. v. Toussaint, T. Dürbeck, K. Schmid, and W. Jacob, *Phys. Scr.* **T145** (2011) 014038.

[4] B. D. Wirth, K. Nordlund, D. G. Whyte, and D. Xu, *MRS Bull.* **36** (2011) 216.

[5] G. R. Longhurst and J. Ambrosec, *Fus. Sci. Technol.* **48** (2005) 468.

[6] R. D. Kolasinski, D. F. Cowgill, and R. A. Causey, *J. Nucl. Mater.* **415** (2011) S676.

[7] D. F. Cowgill, *Fusion Sci. Technol.* **48** (2005) 539.

[8] R. Frauenfelder, *J. Vac. Sci. Technol.* **6** (1969) 388.

[9] W. R. Wampler, *J. Appl. Phys.* **69** (1991) 3063.

[10] F. S. Ham, *J. Phys. Chem. Solids* **6** (1958) 335.

[11] K. E. Brenan, S. L. Campbell, and L. R. Petzhold, *The Numerical Solution of Initial Value Problems in Differential-Algebraic Equations*, SIAM Classics Series, Vol. 14 (1996.)

229 [12] A. Michels, W. De Graaff, T. Wassenaar, J. M. H. Levelt, and P. Louwerse, *Physica*, **25** (1959)
230 25.

231 [13] R. L. Mills, D. H. Liebenberg, J. C. Bronson, and L. C. Schmidt, *J. Chem. Phys.* **66** (1977) 3076.

232 [14] H. K. Mao, A. P. Jephcoat, R. J. Hemley, L. W. Finger, C. S. Zha, R. M. Hazen, and D. E. Cox,
233 *Science* **239** (1989) 1131.

234 [15] C. San Marchi, B. P. Somerday, and S. L. Robinson, *Int. J. Hydrogen Energ.* **32** (2007) 100.

235 [16] M. Tkacz and A. Litwiniuk, *J. Alloys Compd.* **330-332** (2002) 89.

236 [17] G. C. Abell and A. Attalla, *Phys. Rev. Lett.* **59** (1987) 995.

237 [18] A. Van Veen, H. A. Filius, J. De Vries, K. R. Bijerk, G. J. Rozing, and D. Segers, *J. Nucl. Mater.*
238 **155-157** (1988) 1113.

239 [19] J. F. Ziegler, J. P. Biersack, and U. Littmark, *The Stopping and Range of Ions in Solids, Vol. 1*,
240 Pergamon Press, New York (1985).

241 [20] M. Shimada, R. D. Kolasinski, J. P. Sharpe, and R. A. Causey, *Rev. Sci. Instrum.* **82** (2011)
242 083503.

243

Figure Captions

Fig. 1: Comparison between empirical hydrogen equation of state and experimental measurements.

Fig. 2: Comparison of bubble model trapping results with calculations and experiments: (a) temperature variation of fraction of traps filled, (b) retention in 1.5 nm dia. voids as a function of fluence, and (c) concentration contained in voids vs. depth for the experiments of Van Veen et al. [18]. In panel (b), the total retention measured by Van Veen et al. for fluences of 10^{22} m^{-2} and 10^{23} m^{-2} is indicated by the solid markers.

Fig. 3: Surface morphology of (a) ITER-grade and (b) warm-rolled tungsten samples exposed to 100 eV D_2^+. [Irradiation conditions: (a) T_{surf}=350 °C; Φ=1.5×10^{22} $m^{-2}s^{-1}$; F=1.1×10^{26} m^{-2}; (b) T_{surf}=385 °C; Φ=1.1×10^{22} $m^{-2}s^{-1}$; F=0.8×10^{26} m^{-2}]

Figures

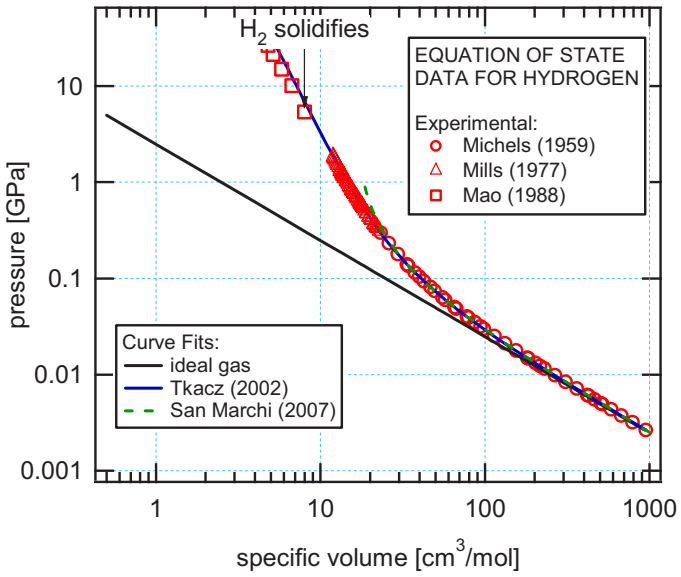

Fig. 1: Comparison between empirical hydrogen equation of state and experimental measurements.

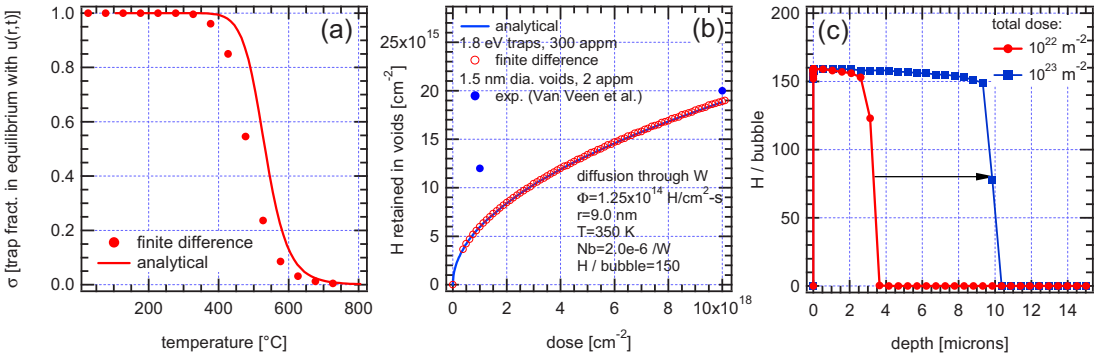

Fig. 2: Comparison of bubble model trapping results with calculations and experiments: (a) temperature variation of fraction of traps filled, (b) retention in 1.5 nm dia. voids as a function of fluence, and (c) concentration contained in voids vs. depth for the experiments of Van Veen et al. [18]. In panel (b), the total retention measured by Van Veen et al. for fluences of 10^{22} m^{-2} and 10^{23} m^{-2} is indicated by the solid markers.

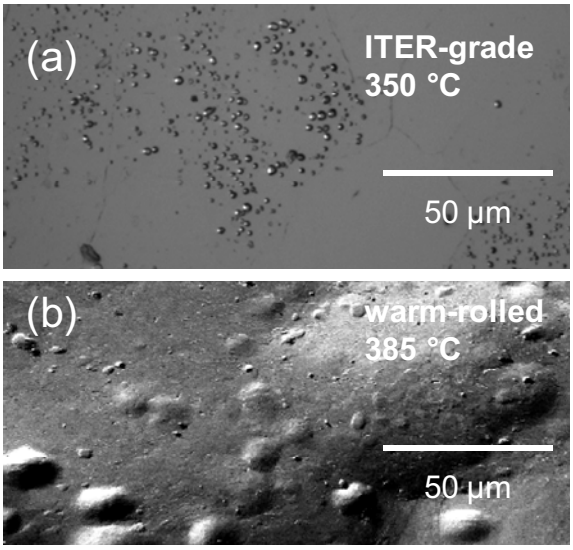

Fig. 3: Surface morphology of (a) ITER-grade and (b) warm-rolled tungsten samples exposed to 100 eV D_2^+. [Irradiation conditions: (a) T_{surf}=350 °C; Φ=1.5×10^{22} m^{-2}s^{-1}; F=1.1×10^{26} m^{-2}; (b) T_{surf}=385 °C; Φ=1.1×10^{22} m^{-2}s^{-1}; F=0.8×10^{26} m^{-2}]